Precision Polyethylene: Changes in Morphology as a Function of Alkyl Branch Size

ARTICLE *in* JOURNAL OF THE AMERICAN CHEMICAL SOCIETY · NOVEMBER 2009

Impact Factor: 12.11 · DOI: 10.1021/ja907521p · Source: PubMed

4 AUTHORS, INCLUDING:

Giovanni Rojas
University ICESI
28 PUBLICATIONS **256** CITATIONS

SEE PROFILE

J|A|C|S
ARTICLES

Published on Web 11/05/2009

Precision Polyethylene: Changes in Morphology as a Function of Alkyl Branch Size

Giovanni Rojas,† Bora Inci, Yuying Wei, and Kenneth B. Wagener*

Center for Macromolecular Science and Engineering, The George and Josephine Butler Polymer Research Laboratory, Department of Chemistry, University of Florida, Gainesville, Florida 32611-7200

Received September 4, 2009; E-mail: wagener@chem.ufl.edu

Abstract: Metathesis polycondensation chemistry has been employed to control the crystalline morphology of a series of 11 precision-branched polyethylene structures, the branch being placed on each 21st carbon and ranging in size from a methyl group to an adamantyl group. The crystalline unit cell is shifted from orthorhombic to triclinic, depending upon the nature of the precision branch. Further, the branch can be positioned either in the crystalline phase or in the amorphous phase of polyethylene, a morphology change dictated by the size of the precision branch. This level of morphology control is accomplished using step polymerization chemistry to produce polyethylene rather than conventional chain polymerization techniques. Doing so requires the synthesis of a series of unique symmetrical diene monomers incorporating the branch in question, followed by ADMET polymerization and hydrogenation to yield the precision-branched polyethylene under study. Exhaustive structure characterization of all reaction intermediates as well as the precision polymers themselves is presented. A clear change in morphology was observed for such polymers, where small branches (methyl and ethyl) are included in the unit cell, while branches equal to or greater in mass than propyl are excluded from the crystal. When the branch is excluded from the unit cell, all such polyethylene polymers possess essentially the same melting temperature, regardless of the size of the branch, even for the adamantyl branch.

Introduction

Given that polyethylene (PE) is the most widely consumed macromolecule today, its structure remains of scientific interest in spite of the vast amount of research already present in the literature. The ability to produce materials with a wide range of polymer architectures is a result of systematically altering the morphology of this polyolefin.[1,2] Improvements to the performance of polyethylene can be achieved by controlling the mode of polymerization, catalyst type, pressure, and temperature. These manipulations can alter the amount of short-chain branching (SCB) and the short-chain branch distribution (SCBD) to tune the final properties like tensile strength, stiffness, processability, and melting temperature.[1,2] Linear low-density polyethylene (LLDPE) structures are of particular interest. These are copolymers of ethylene and α-olefins, where the short chain branch is delivered by the α-olefin comonomer. Propene, 1-butene, 1-hexene, and 1-octene are the comonomers of choice due to their low cost and their well understood effects on the thermal and mechanical properties of the final material.[2−12]

Commercial LLDPE is prepared by chain-growth polymerization using Ziegler−Natta or metallocene chemistry.[13] The absence of multisite initiation in single-site metallocene systems results in the synthesis of copolymers possessing narrower molecular weight distributions and higher levels of α-olefin comonomer incorporation.[14,15] Due to the well-defined nature of the catalyst, metallocene systems produce materials incorporating linear and bulky α-olefins not compatible with Ziegler−Natta chemistry. Copolymerization via metallocene chemistry of ethylene with odd-carbon-number α-olefins (e.g., 1-pentene or 1-heptene) is also feasible, because such compounds are available using the Fischer−Tropsch olefin synthesis process. These possibilities have led to the creation of a significant number of ethylene/α-olefin copolymers with a wide

† Present address: Max Planck Institute for Polymer Research, Mainz, Germany, 55128.

(1) Muller, A. J.; Hernandez, Z. H.; Arnal, M. L.; Sanchez, J. J. *Polym. Bull.* **1997**, *39*, 465–472.
(2) Czaja, K.; Sacher, B.; Bialek, M. *J. Therm. Anal. Calorim.* **2002**, *67*, 547–554.
(3) Anantawaraskul, S.; Soares, J. B. P.; Jirachaithorn, P. *Macromol. Symp.* **2007**, *257*, 94–102.
(4) Alobaidi, F.; Ye, Z. B.; Zhu, S. P. *J. Polym. Sci., Part A: Polym. Chem.* **2004**, *42*, 327–4336.
(5) Seger, M. R.; Maciel, G. E. *Anal. Chem.* **2004**, *76*, 5734–5747.
(6) Pracella, M.; D'Alessio, A.; Giaiacopi, S.; Galletti, A. R.; Carlini, C.; Sbrana, G. *Macromol. Chem. Phys.* **2007**, *208*, 1560–1571.
(7) Hsieh, E. T.; Randall, J. C. *Macromolecules* **1982**, *15*, 1402–1406.
(8) Haigh, J. A.; Nguyen, C.; Alamo, R. G.; Mandelkern, L. *J. Therm. Anal. Calorim.* **2000**, *59*, 435–450.
(9) Jokela, K.; Vaananen, A.; Torkkeli, M.; Starck, P.; Serimaa, R.; Lofgren, B.; Seppala, J. *J. Polym. Sci., Part B: Polym. Phys.* **2001**, *39*, 1860–1875.
(10) Ungar, G.; Zeng, K. B. *Chem. Rev.* **2001**, *101*, 4157–4188.
(11) Starck, P.; Malmberg, A.; Lofgren, B. *J. Appl. Polym. Sci.* **2002**, *83*, 1140–1156.
(12) Wright, K. J.; Lesser, A. J. *Macromolecules* **2001**, *34*, 3626–3633.
(13) Peacock, A. J. *Handbook of Polyethylene: Structures, Properties, and Applications*;Marcel Dekker: New York, 2000; 534 pp.
(14) Schneider, M. J.; Mülhaupt, R. *J. Mol. Catal. A: Chem.* **1995**, *101*, 11–16.
(15) Suhm, J.; Schneider, M. J.; Mulhaupt, R. *J. Mol. Catal. A: Chem.* **1998**, *128*, 215–227.

10.1021/ja907521p CCC: $40.75

range of applications.[16−24] Furthermore, metallocene copolymerization of ethylene with nonlinear, bulkier α-olefins such as 3-methyl-1-butene,[25−28] 4-methyl-1-pentene,[29−32] vinylcyclohexene,[33−36] and norbornene[28] has created a new class of materials with better impact strength than that of traditional ethylene linear α-olefin copolymers.

By its nature, copolymerization of ethylene with α-olefins via chain-propagation chemistry incorporates structural defects via head-to-head or tail-to-tail monomer coupling. Further, inevitable chain transfer or chain walking produces structures with alkyl branches of varying lengths randomly spaced along the main chain.[37−41]

In recent years, we have obviated formation of these defects by turning to step polycondensation chemistry (the ADMET reaction) rather than chain polymerization chemistry.[42] Symmetrical diene monomers are condensed into unsaturated polymers which upon hydrogenation generate what we call "precision-branched polyethylene". We are able to create polymers where both the identity of the branch and its position along the chain are known without equivocation. We are also able to systematically "randomize" the position of the branch to mirror "reality" in commercial polymer systems. Note that we have made *unbranched* ADMET polyethylene to serve as a point of comparison with chain-made commercial polyethylene. The thermal behavior of this ADMET polyethylene is virtually the same as that of high-density polyethylene (T_m = 134 °C, Δh_m = 204 J/g).[55] The crystalline unit cell is orthorhombic. A most probable distribution of molecular weights exists, and M_w values approaching 80 000 can be achieved in this way.

The key synthetic point in this approach revolves around the synthesis of appropriate symmetrical diene monomers. In order to ensure absolute control of branch identity and its precision placement along the polymer backbone, the branch is "built-in" the diene monomer itself before polymerization. Homopolymerization of the diene monomer (via polycondensation), followed by exhaustive hydrogenation, generates a symmetrical repeat unit, which in effect mirrors a precision model ethylene/α-olefin copolymer under examination.

Precisely placed methyl branches in ADMET PE were the first to be examined.[43] Continuation of this research led to the synthesis of ethyl-branched polyethylene[44] and subsequently to the creation of butyl- and hexyl-branched polyethylene.[45,46] This paper extends the study to branches of different mass for comparative purposes, where we have observed a significant change in polymer morphology as a function of branch size. We report the synthesis, characterization, thermal behavior, and X-ray investigation of polyethylene containing 11 different branches, each placed on every 21st carbon in polyethylene.

Results and Discussion

A. Monomer Synthesis and ADMET Polymerization of Precisely Sequenced Polymers. Monomer synthesis is key in this research, where earlier efforts employed elaborate methodologies for the synthesis of α,ω-dienes in only moderate yields.[43−45] Lately, we have been able to synthesize symmetrical α,ω-diene monomers possessing alkyl branches of various lengths in two steps with nearly quantitative yields via the alkylation/decyanation of primary nitriles. This approach is based on the double alkenylation of the carbon α to the nitrile, followed by the reductive elimination of the nitrile moiety. Scheme 1 shows the synthetic approach for the preparation of alkyl α,ω-diene monomers (**4a**−**k**) from primary nitriles **2a**−**k**, where the ease of monomer synthesis has allowed us to expand the scope of our study significantly. While most of nitriles were commercially available, nitriles **2i** and **2j** were synthesized by cyanation of bromides **1i** and **1j**.

Alkenylation of nitriles **2a**−**k** in the presence of lithium diisopropyl amide (LDA) and 11-bromoundec-1-ene produces the alkylcyano α,ω-dienes **3a**−**k** in quantitative yields. Decyanation of nitriles **3a**−**k** is achieved with potassium metal via radical chemistry. The resulting tertiary radical after decyanation is further quenched by abstraction of hydrogen from *t*-BuOH to give α,ω-diene monomers **4a**−**k** in quantitative yields.

Scheme 2 illustrates the ADMET polycondensation of alkyl α,ω-diolefin monomers **4a**−**k** using first-generation Grubbs catalyst (**5**). Typical polycondensation procedures are used (no solvent, high vacuum, preferably using mechanical stirring in the reactor). The polymerization proceeds efficiently, yielding 11 unsaturated polymers with branches of methyl to adamantyl on every 21st carbon. Exhaustive hydrogenation of the unsaturated polymers using *p*-toluenesulfonyl hydrazide, tripropyl amine, and xylene yields saturated ADMET polymers. As described further below, the efficiency of hydrogenation can

(16) Da Silva, M. A.; Galland, G. B. *J. Polym. Sci. Part A: Polym. Chem.* **2008**, *46*, 947–957.
(17) Luruli, N.; Heinz, L.-C.; Grumel, V.; Brüll, R.; Pasch, H.; Raubenheimer, H. G. *Polymer* **2006**, *47*, 56–66.
(18) Halasz, L.; Belina, K.; Vorster, O. C.; Juhasz, P. *Plastics, Rubber Compos.* **2004**, *33*, 205–211.
(19) Neves, C. J.; Monteiro, E.; Habert, A. C. *J. Appl. Polym. Sci.* **1993**, *50*, 817–824.
(20) Luruli, N.; Pijpers, T.; Brull, R.; Grumel, V.; Pasch, H.; Mathot, V. *J. Polym. Sci., Part B: Polym. Phys.* **2007**, *45*, 2956–2965.
(21) Halasz, L.; Vorster, O. *Polym. Adv. Technol.* **2006**, *17*, 1004–1008.
(22) Joubert, D. J.; Goderis, B.; Reynaers, H.; Mathot, V. B. F. *J. Polym. Sci., Part B: Polym. Phys.* **2005**, *43*, 3000–3018.
(23) Joubert, D.; Tincul, I. *Macromol. Symp.* **2002**, *178*, 69–79.
(24) Tincul, I.; Smith, J.; van Zyl, P. *Macromol. Symp.* **2003**, *193*, 13–28.
(25) Derlin, S.; Kaminsky, W. *Macromolecules* **2007**, *40*, 4130–4137.
(26) Kirshenb., I.; Feist, W. C.; Isaacson, R. B. *J. Appl. Polym. Sci.* **1965**, *9*, 3023–3031.
(27) Endo, K.; Fujii, K.; Otsu, T. *J. Polym. Sci. Part A: Polym. Chem.* **1991**, *29*, 1991–1993.
(28) Kaminsky, W.; Beulich, I.; Arndt-Rosenau, M. *Macromol. Symp.* **2001**, *173*, 211–225.
(29) Mauler, R. S.; Galland, G. B.; Scipioni, R. B.; Quijada, R. *Polym. Bull.* **1996**, *37*, 469–474.
(30) Losio, S.; Tritto, I.; Zannoni, G.; Sacchi, M. C. *Macromolecules* **2006**, *39*, 8920–8927.
(31) Irwin, L. J.; Reibenspies, J. H.; Miller, S. A. *J. Am. Chem. Soc.* **2004**, *126*, 16716–16717.
(32) Xu, G.; Cheng, D. *Macromolecules* **2001**, *34*, 2040–2047.
(33) Aitola, E.; Puranen, A.; Setala, H.; Lipponen, S.; Leskela, M.; Repo, T. *J. Polym. Sci. Part A: Polym. Chem.* **2006**, *44*, 6569–6574.
(34) Nomura, K.; Itagaki, K. *Macromolecules* **2005**, *38*, 8121–8123.
(35) Gendler, S.; Groysman, S.; Goldschmidt, Z.; Shuster, M.; Kol, M. *J. Polym. Sci. Part A: Polym. Chem.* **2006**, *44*, 1136–1146.
(36) Starck, P.; Lofgren, B. *J. Macromol. Sci.-Phys.* **2002**, *B41*, 579–597.
(37) Carella, J. M.; Graessley, W. W.; Fetters, L. J. *Macromolecules* **1984**, *17*, 2775–2786.
(38) Gotro, J. T.; Graessley, W. W. *Macromolecules* **1984**, *17*, 2767–2775.
(39) Colby, R. H.; Milliman, G. E.; Graessley, W. W. *Macromolecules* **1986**, *19*, 1261–1262.
(40) Morton, M.; Clarke, R. G.; Bostick, E. E. *J. Polym. Sci. Part A: Gen. Pap.* **1963**, *1*, 475–482.
(41) Krishnamoorti, R.; Graessley, W. W.; Balsara, N. P.; Lohse, D. J. *Macromolecules* **1994**, *27*, 3073–3081.
(42) O'Gara, J. E.; Wagener, K. B. *Makromol. Chem., Rapid Commun.* **1993**, *14*, 657–662.
(43) Smith, J. A.; Brzezinska, K. R.; Valenti, D. J.; Wagener, K. B. *Macromolecules* **2000**, *33*, 3781–3794.
(44) Sworen, J. C.; Smith, J. A.; Berg, J. M.; Wagener, K. B. *J. Am. Chem. Soc.* **2004**, *126*, 11238–11246.
(45) Sworen, J. C.; Wagener, K. B. *Macromolecules* **2007**, *40*, 4414–4423.
(46) Rojas, G.; Wagener, K. B. *Macromolecules* **2009**, *42*, 1934–1937.

Scheme 1. Synthesis of 12-Alkyltricosa-1,22-dienes (**4a**−**k**)

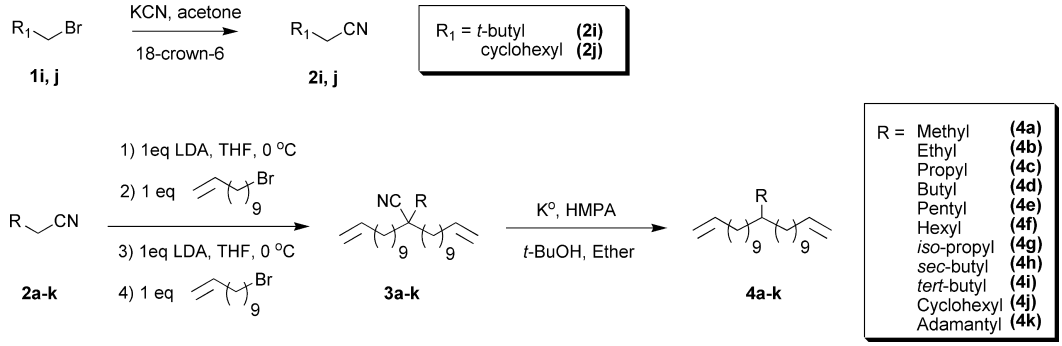

Scheme 2. Synthesis of Precisely Sequenced Polymers

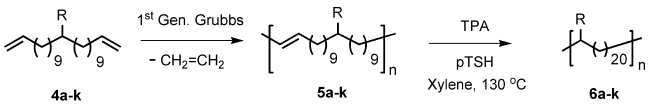

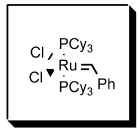

1st Generation Grubbs catalyst
5

Unsaturated polymer	Branch (R)	Saturated polymer
5a	Methyl	6a
5b	Ethyl	6b
5c	Propyl	6c
5d	Butyl	6d
5e	Pentyl	6e
5f	Hexyl	6f
5g	*iso*-propyl	6g
5h	*sec*-butyl	6h
5i	*tert*-butyl	6i
5j	Cyclohexyl	6j
5k	Adamantyl	6k

Table 1. Molecular Weights and Thermal Data for Precisely Sequenced Polymers

branch identity on every 21st carbon	T_m, °C (peak)	Δh_m, J/g	$\bar{M}_w \times 10^3$ (PDI)[b]	
			unsaturated[a]	saturated[a]
methyl	63	104	20.2 (1.7)	20.2 (1.7)
ethyl	24	65	50.2 (1.9)	50.7 (1.9)
propyl	12	60	41.2 (1.7)	41.4 (1.7)
butyl	12	57	41.5 (1.8)	40.3 (1.7)
pentyl	14	58	45.1 (1.8)	45.8 (1.8)
hexyl	12	49	44.6 (1.8)	46.1 (1.7)
isopropyl	11	37	45.5 (1.7)	46.0 (1.7)
sec-butyl	9	43	43.0 (1.6)	42.6 (1.9)
tert-butyl	13	50	30.6 (1.7)	32.1 (1.7)
cyclohexyl	9	37	32.5 (1.6)	33.6 (1.6)
adamantyl	−8 and 17	2 and 8	64.7 (1.7)	70.8 (1.3)

[a] Weight-average molecular weight data obtained by GPC in THF (40 °C) relative to polystyrene standards (g/mol). [b] PDI, polydispersity index ($\bar{M}_w/\bar{M}_n$).

be followed by the disappearance of the olefin signals in ^{1}H NMR (Figure 1) and ^{13}C NMR (Figure 2) and by the absence of the out-of-plane alkene C−H bend (969 cm^{-1}) using infrared (IR) spectroscopy (Figure 4).

Table 1 reports the molecular weights for the precisely sequenced polymers obtained via ADMET polymerization; weight-average molecular weights were obtained by gel permeation chromatography (GPC) versus polystyrene standards with molecular weights of sufficient mass to allow analysis of thermal behavior. As expected, most probable molecular weight distributions are observed. Important to note is that the molecular weights before and after hydrogenation show that no cleavage of the polymer chains occurs during hydrogenation.[43]

B. Structural Data for Precisely Sequenced Polymers. This synthetic approach produces polymers with precisely known primary structures,[43−45] meaning that the polymers only have defects (branches) intentionally and evenly placed along the main chain. Examination of ^{1}H and ^{13}C NMR spectra of monomers and polymers confirms complete transformation and control over the primary structure's precision.

As an example of this level of control, Figure 1 shows the ^{1}H NMR spectra for the ADMET polymer **6i-(*tert*-butyl)** and its precursors. The transformation begins with the cyanation of 1-bromo-2,2-dimethylpropane (**1i**), yielding 3,3-dimethylbutanenitrile (**2i**), shown in Figure 1a. Double alkenylation of nitrile **2i** with 11-bromoundec-1-ene yields premonomer **3i**, 2-*tert*-butyl-2-(undec-10-enyl)tridec-12-enenitrile, as shown in Figure 1b. Decyanation of nitrile **3i** forms monomer **4i**, 12-*tert*-butyltricosa-1,22-diene, in quantitative yield, as shown in Figure 1c. ADMET polymerization of **4i** yields the unsaturated polymer, **5i-(*tert*-butyl)**. Analysis of the olefin region (5−6 ppm) supports formation of polymer, which is evidenced by the disappearance of the terminal olefin signals (5.1 and 5.9 ppm in Figure 1c) and the formation of the internal olefin (5.3 ppm in Figure 1d). Further hydrogenation of the internal olefins yields **6i-(*tert*-butyl)**, a perfectly sequenced polymer, corresponding to polyethylene with *tert*-butyl branches on every 21st backbone carbon, with no observable traces of olefin by ^{1}H NMR (Figure 1e).

Figure 2 shows the ^{13}C NMR spectra for the same transformations. In the spectrum for the 3,3-dimethylbutanenitrile (**2i**, Figure 2a), the resonance at 118.67 shows the presence of the nitrile functionality. After the double alkenylation of nitrile **2i**, the spectrum for 2-*tert*-butyl-2-(undec-10-enyl)tridec-12-enenitrile (**3i**, Figure 2b) shows the presence of the nitrile functionality at 122.95 ppm along with the characteristic terminal olefin signals at 114.27 and 139.26 ppm, respectively. The absence of the signal at 122.95 ppm after decyanation (Figure 2c) demonstrates complete elimination of the CN group, yielding monomer **4i**, 12-*tert*-butyltricosa-1,22-diene. ADMET polymerization of **4i** yields the unsaturated polymer **5i-(*tert*-butyl)**. Comparison of parts c and d of Figure 2 shows the disappearance of the signals belonging to the terminal olefin at 114.31 and 139.44 ppm and formation of the new internal olefin (cis at 130.12 ppm, minor component, and trans at 130.58 ppm, major component) produced from the effective metathesis polymerization. Subsequent exhaustive hydrogenation of the internal olefin yields the saturated polymer **6i-(*tert*-butyl)**, whose ^{13}C NMR spectrum (Figure 2e) shows no detectable trace of olefins. This observation is further supported by the absence of the out-of-plane C−H bend in the alkene region at 969 cm^{-1} in the infrared (IR) spectrum, as described below.

Upon close inspection of the ^{13}C NMR data for the ADMET polymers, it can be concluded that the branches are precisely placed along the polyethylene main backbone with no unwanted "defects" due to chain transfer typically observed during chain-

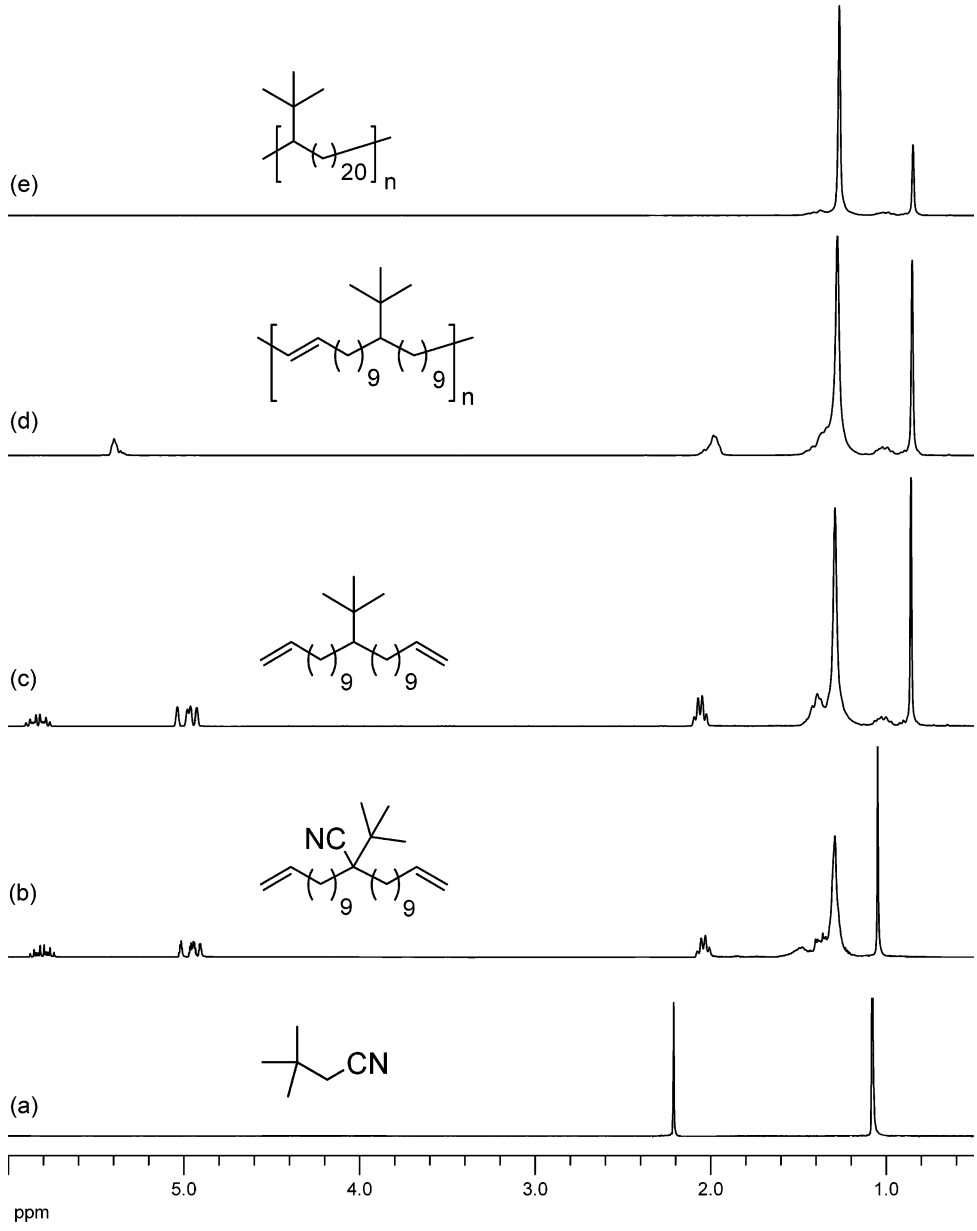

Figure 1. Comparison of ^{1}H NMR spectra for a typical ADMET polymerization transformation **6i-(*tert*-butyl)**: (a) 3,3-dimethylbutanenitrile (**2i**); (b) premonomer **3i**, 2-*tert*-butyl-2-(undec-10-enyl)tridec-12-enenitrile; (c) monomer **4i**, 12-*tert*-butyltricosa-1,22-diene; (d) ADMET unsaturated polymer **5i-(*tert*-butyl)**; and (e) ADMET saturated polymer **6i-(*tert*-butyl)**.

growth chemistry. Figure 3 shows a portion (10−55 ppm) of the ^{13}C NMR spectra for some of the precisely sequenced polymers, **6c-(propyl)**, **6e-(pentyl)**, **6g-(*iso*-propyl), 6i-(*tert*-butyl)**, and **6j-(cyclohexyl)**. All spectra are dominated by a singlet at 29.99 ppm corresponding to methylenes on the main polyethylene chain. Note that the presence of alkyl branches precisely placed along the main chain affects the chemical shifts of carbons located within three CH_2 units from an individual branch.[47] In the spectrum for **6c-(propyl)**, which is polyethylene containing propyl branches on every 21st backbone carbon (Figure 3a), the resonances belonging to the propyl branch, 1 (δ 14.80 ppm), 2 (δ 20.07 ppm), 3 (δ 36.37 ppm), and the carbon at the branch point 4 (δ 37.42 ppm) indicate that only propyl branches are present, in agreement with previously reported data on chain-growth materials obtained by copolymerization of ethylene with 1-pentene.[17,48−51] While the **6c-(propyl)** spectrum shows resonances for three carbons at the propyl branch, the **6e-(pentyl)** spectrum, Figure 3b, shows five resonances corresponding to the pentyl branch precisely placed on every 21st backbone carbon: a (δ 14.80 ppm), b (δ 22.97 ppm), c (δ 26.62 ppm), d (δ 26.94 ppm), and e (δ 33.89 ppm). In agreement with the **6c-(propyl)** spectrum, which shows a resonance for the branch point carbon at 37.42 ppm, **6e-(pentyl)** shows the corresponding branch-point peak at 37.64 ppm.[21−24]

(47) Sworen, J. C.; Smith, J. A.; Wagener, K. B.; Baugh, L. S.; Rucker, S. P. *J. Am. Chem. Soc.* **2003**, *125*, 2228–2240.

(48) Blitz, J. P.; Mcfaddin, D. C. *J. Appl. Polym. Sci.* **1994**, *51*, 13–20.

(49) Randall, J. C. *J. Polym. Sci. Part B: Polym. Phys.* **1973**, *11*, 275–287.

(50) Striegel, A. M.; Krejsa, M. R. *J. Polym. Sci., Part B: Polym. Phys.* **2000**, *38*, 3120–3135.

(51) Sarzotti, D. M.; Soares, J. B. P.; Penlidis, A. *J. Polym. Sci., Part B: Polym. Phys.* **2002**, *40*, 2595–2611.

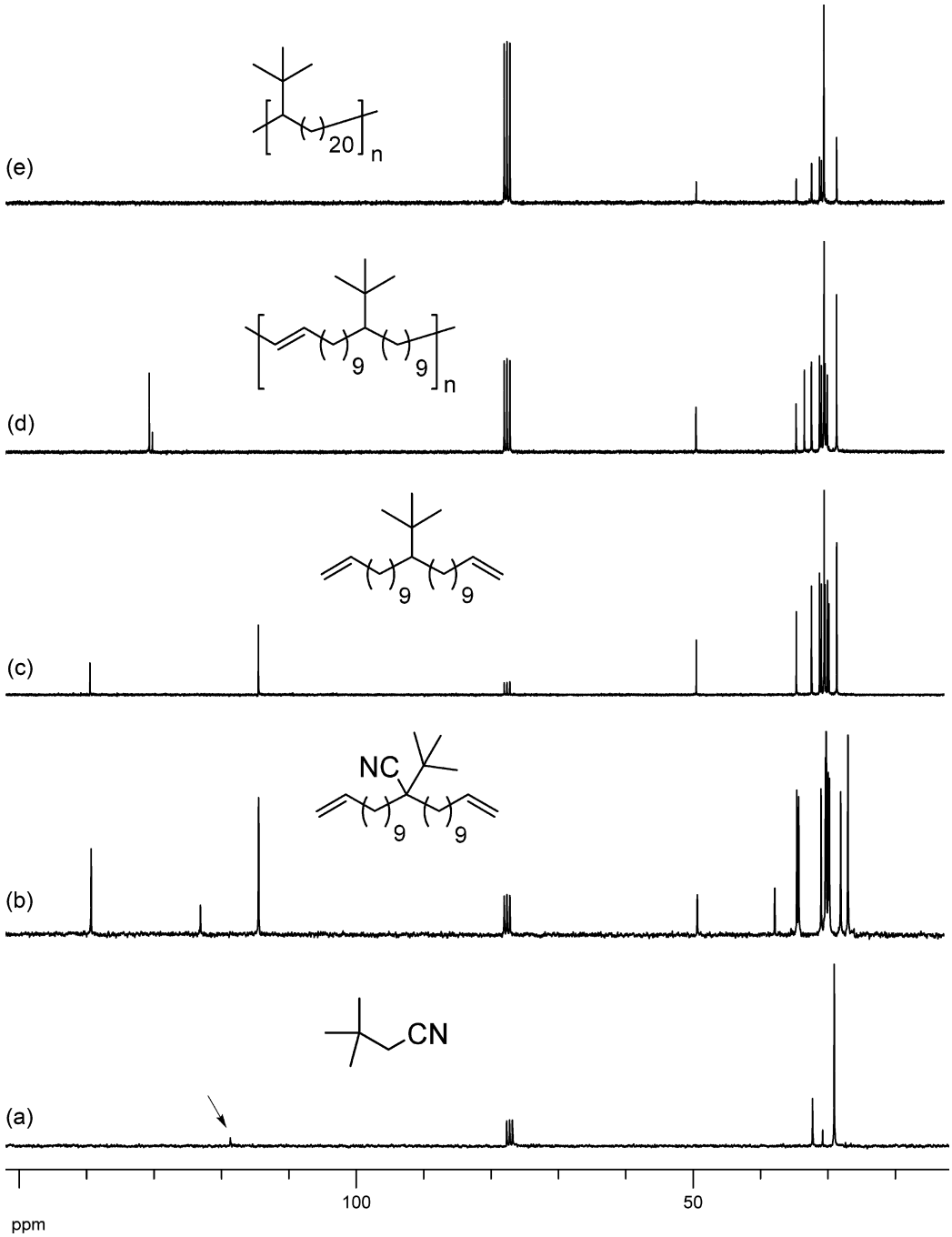

Figure 2. Comparison of ^{13}C NMR spectra for a typical ADMET polymerization transformation **6i-(*tert*-butyl)**: (a) 3,3-dimethylbutanenitrile (**2h**); (b) premonomer **3h**, 2-*tert*-butyl-2-(undec-10-enyl)tridec-12-enenitrile; (c) monomer **4h**, 12-*tert*-butyltricosa-1,22-diene; (d) ADMET unsaturated polymer **5i-(*tert*-butyl)**; and (e) ADMET saturated polymer **6i-(*tert*-butyl)**.

In addition to spectra a and b of Figure 3 for polyethylene with precisely placed linear branches, spectra c−e of Figure 3 present the ^{13}C NMR spectra for polyethylene containing nonlinear bulkier branches on every 21st carbon. **6g-(*iso*-propyl)**, **6i-(*tert*-butyl)**, and **6j-(cyclohexyl)** are shown; **6h-(*sec*-butyl)** and **6k-(adamantly)** were omitted for better clarity. In all cases, the resonances belonging to the branches, as well as the resonance from the carbon at the branch point, indicate that only intentionally placed branches are present. Peak assignments were based on previous detailed NMR studies.[25−36,52−63]

It is not surprising that the presence of a bulkier branch, for example isopropyl, causes a shift in the resonance corresponding to the carbon at the branch point, 37.42 and 37.64 ppm for the carbons at propyl and pentyl branches, respectively, versus 43.96 ppm for the carbon directly attached to an isopropyl branch. The resonances for the backbone carbon at all nonlinear branches were shifted, due to the highly branched functionalization, as shown in Figure 3.

In addition to the NMR characterization of the precisely sequenced ADMET materials, infrared (IR) spectroscopy was used to study all precision polymers. Although X-ray diffraction techniques provide the absolute crystal structure, IR spectroscopy is a complementary technique that provides an estimation of the crystal structure. Tashiro et al. carried out a study of branching behavior on polyethylene using wide-angle X-ray diffraction (WAXD), IR, and Raman spectroscopy. They

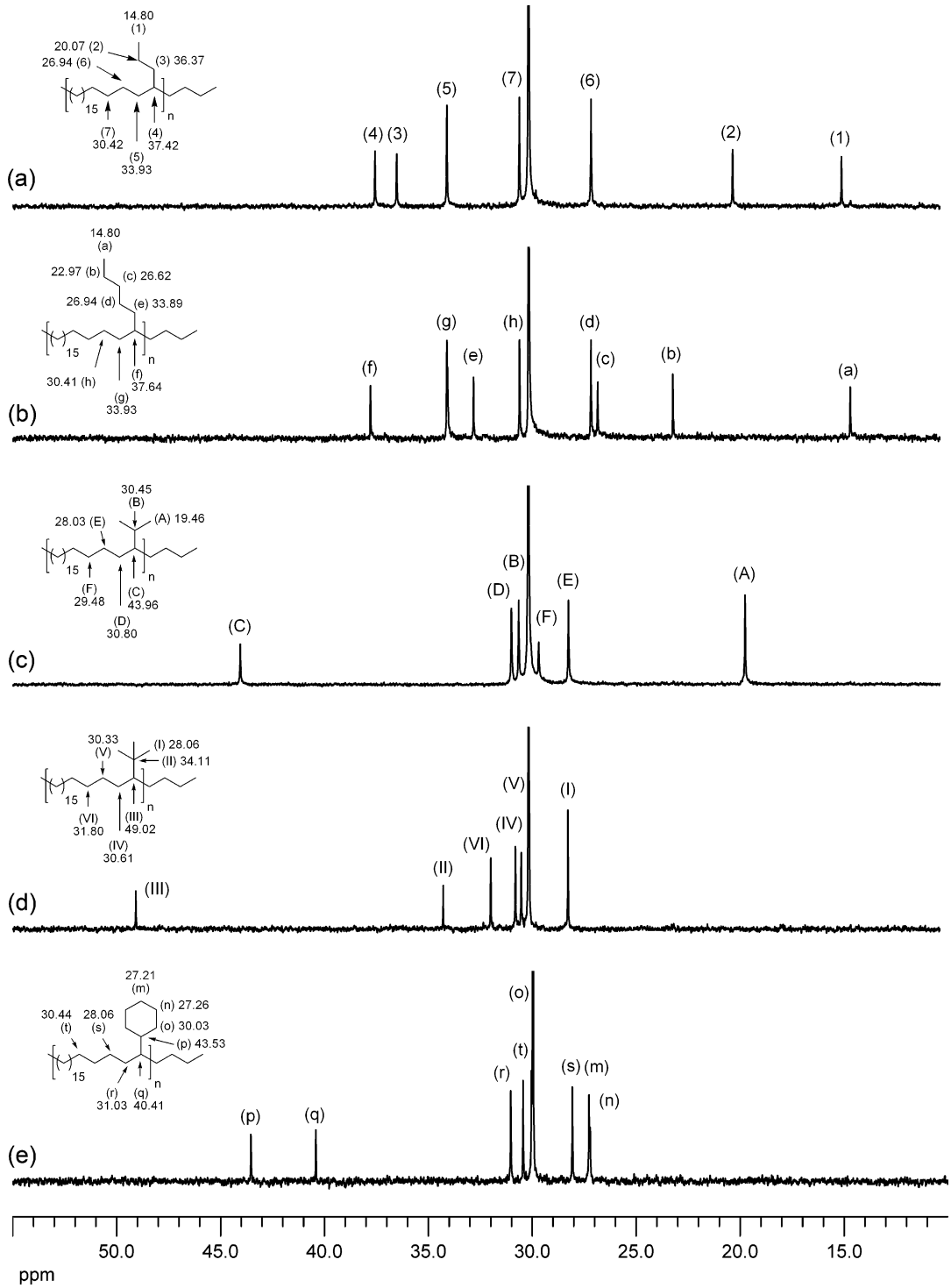

Figure 3. Comparison of ^{13}C NMR spectra for a typical ADMET polymerization transformation possessing bulky branches: (a) **6c-(propyl)**, (b) **6e-(pentyl)**, (c) **6g-(*iso*-propyl)**, (d) **6i-(*tert*-butyl)**, (e) **6j-(cyclohexyl)**. **6h-(*sec*-butyl)** and **6k-(adamantyl)** were omitted for a better figure presentation.

concluded that the scissoring at 1466 cm^{-1} and the methylene rock at 721 cm^{-1} indicate a hexagonal crystal structure, while the double methylene rock at 719 and 730 cm^{-1} and single band at 1471 cm^{-1} correspond to an orthorhombic crystal structure.[6,64,65]

Figure 4 shows the IR spectra for the **6c-(propyl)**, **6e-(pentyl)**, **6g-(*iso*-propyl)**, **6h-(*sec*-butyl)**, **6i-(*tert*-butyl)**, **6j-(cyclohexyl)**, and **6k-(adamantyl)** polymers, with the spectra of previously reported precisely sequenced ones, **6a-(methyl)**,[43] **6b-(ethyl)**,[44] **6f-(hexyl)**,[45] and **6d-(butyl)**,[46] included for comparison. As mentioned above, there is no out-of-plane C−H bend absorption at 969 cm^{-1}, indicating complete absence of C═C in the saturated polymers. All spectra are dominated by two sets of absorption bands (~2900 and 1472 cm^{-1}) belonging to C−H stretching and methylene scissoring, respectively. In addition to the stretching and scissoring, the methylene rocking band is observed for all copolymers at 718 cm^{-1}, which is often associated with the monoclinic crystalline structure.[66] Although orthorhombic crystals show the characteristic Davidov splitting around 720 cm^{-1},[64,65] all of our precisely sequenced ADMET polymers display a single absorption band at 718 cm^{-1},

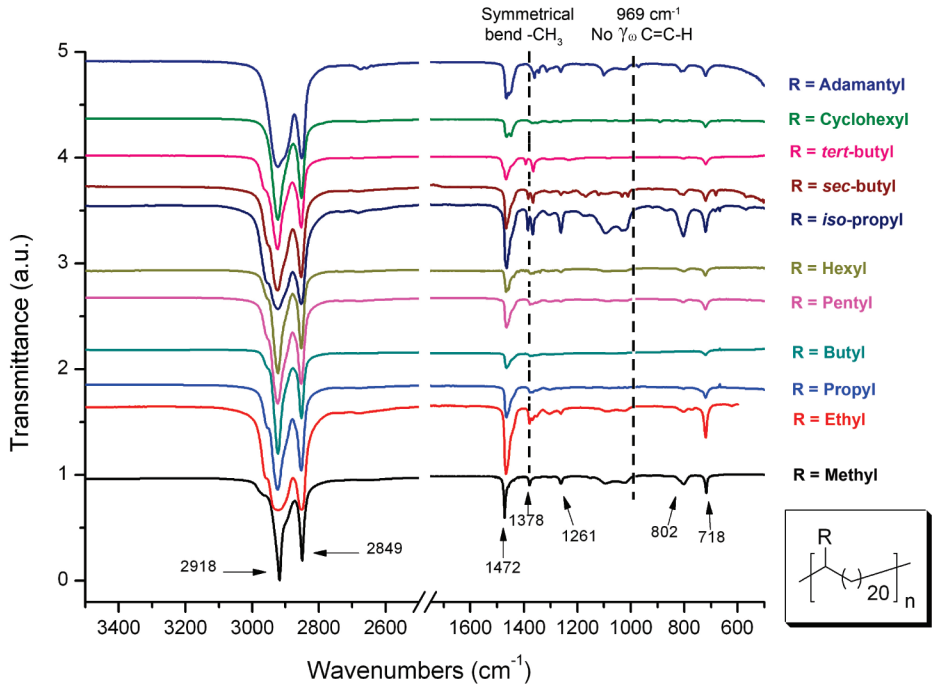

Figure 4. Infrared spectra for the saturated ADMET polymers **6a-(methyl)**, **6b-(ethyl)**, **6c-(propyl)**, **6d-(butyl)**, **6e-(pentyl)**, **6f-(hexyl)**, **6g-(*iso*-propyl)**, **6h-(*sec*-butyl)**, **6i-(*tert*-butyl)**, **6j-(cyclohexyl)**, and **6k-(adamantyl)**.

indicating the absence of orthorhombic crystal behavior. This is a direct result of the branch being present. Moreover, the two experimental absorption bands at 718 and 1472 cm^{-1} are characteristic of a highly disordered phase, similar to the pattern previously observed.[43−45] Comparison of all spectra in Figure 4 suggests that incorporation of linear defects (methyl to hexyl) and nonlinear bulkier branches (*iso*-propyl, *sec*-butyl, *tert*-butyl, cyclohexane, and adamantyl) evenly spaced along the polyethylene chain does not alter the C−H stretching or methylene scissoring and methylene rocking regions in the IR. However, there is significant variation in the intensity of the absorption band at 1378 cm^{-1}, corresponding to the symmetrical bend for the terminal methyls on the pendant branches. As Figure 4 shows, the intensity of the absorption band at 1378 cm^{-1} is smaller when linear alkyl branches are incorporated, while higher intensity is observed when bulkier branches (*iso*-propyl, *sec*-butyl, and *tert*-butyl) are placed along the PE chain. On the other hand, when cyclohexyl and adamantyl groups are precisely placed on every 21st backbone carbons, the absorption at 1378 cm^{-1} almost disappears because of the absence of methyl groups at the branch; the very weak absorption at 1378 cm^{-1} is due to the terminal methyl groups of the PE backbone of **6j-(cyclohexyl)** and **6k-(adamantyl)**.

C. Thermal Behavior for Precisely Sequenced Polymers. Numerous thermal studies have been performed on commercially produced chain-growth LLDPE,[11,36,67−71] as well as for ADMET-produced random and precisely sequenced linear low-density PEs (LLDPE).[43−45,47,72−76] Those studies showed that the melting behavior of ethylene-based copolymers is influenced by the amount of short-chain branching (SCB), where the determining factor on the final physical properties of the resulting LLDPE is the short-chain-branch distribution (SCBD). Interpretation of such thermal results for chain-growth PE has

(52) Lindeman, L. P.; Adams, J. Q. *Anal. Chem.* **1971**, *43*, 1245–1252.
(53) Borriello, A.; Busico, V.; Derosa, C.; Schulze, D. *Macromolecules* **1995**, *28*, 5679–5680.
(54) Asakura, T.; Nakayama, N. *Polym. Commun.* **1991**, *32*, 213–216.
(55) Randall, J. C. *J. Polym. Sci. Part B: Polym. Phys.* **1975**, *13*, 1975–1990.
(56) Keaton, R. J.; Jayaratne, K. C.; Henningsen, D. A.; Koterwas, L. A.; Sita, L. R. *J. Am. Chem. Soc.* **2001**, *123*, 6197–6198.
(57) Zambelli, A.; Ammendola, P.; Locatelli, P.; Sacchi, M. C. *Macromolecules* **1984**, *17*, 977–978.
(58) Carlini, C.; Altomare, A.; Menconi, F.; Ciardelli, F. *Macromolecules* **1987**, *20*, 464–465.
(59) Oliva, L.; Longo, P.; Zambelli, A. *Macromolecules* **1996**, *29*, 6383–6385.
(60) Sacchi, M. C.; Barsties, E.; Tritto, I.; Locatelli, P.; Brintzinger, H. H.; Stehling, U. *Macromolecules* **1997**, *30*, 1267–1271.
(61) Zambelli, A.; Ammendola, P.; Sacchi, M. C.; Locatelli, P.; Zannoni, G. *Macromolecules* **1983**, *16*, 341–348.
(62) Kobayashi, S.; Kataoka, H.; Ishizone, T.; Kato, T.; Ono, T.; Kobukata, S.; Arimoto, K.; Ogi, H. *React. Funct. Polym.* **2009**, *69*, 409–415.
(63) Zuanic, M.; Majerski, Z.; Janovic, Z. *J. Polym. Sci. Part C: Polym. Lett.* **1981**, *19*, 387–389.
(64) Tashiro, K.; Sasaki, S.; Kobayashi, M. *Macromolecules* **1996**, *29*, 7460–7469.
(65) Rueda, D. R.; Baltacalleja, F. J.; Hidalgo, A. *J. Polym. Sci., Part B: Polym. Phys.* **1977**, *15*, 2027–2031.
(66) Kang, N.; Xu, Y. Z.; Cai, Y. L.; Li, W. H.; Weng, S. F.; Feng, W.; He, L. T.; Xu, D. F.; Wu, J. G.; Xu, G. X. *J. Mol. Struct.* **2001**, *562*, 19–24.
(67) Wilfong, D. L.; Knight, G. W. *J. Polym. Sci. Part B: Polym. Phys.* **1990**, *28*, 861–870.
(68) Starck, P. *Polym. Int.* **1996**, *40*, 111–122.
(69) Starck, P.; Rajanen, K.; Lofgren, B. *Thermochim. Acta* **2003**, *395*, 169–181.
(70) McKenna, T. F. *Eur. Polym. J.* **1998**, *34*, 1255–1260.
(71) Mirabella, F. M. *J. Polym. Sci., Part B: Polym. Phys.* **2001**, *39*, 2800–2818.
(72) Rojas, G.; Berda, E. B.; Wagener, K. B. *Polymer* **2008**, *49*, 2985–2995.
(73) Rojas, G.; Wagener, K. Precision Polyolefin Structure: Modeling Polyethylene Containing Methyl and Ethyl Branches. In *Metathesis Chemistry*; Springer: Dordrecht, The Netherlands, 2007; pp 305−324.
(74) Baughman, T. W.; Sworen, J. C.; Wagener, K. B. *Macromolecules* **2006**, *39*, 5028–5036.
(75) Baughman, T. W.; Wagener, K. B. *Metathesis Polym.* **2005**, *176*, 1–42.
(76) Berda, E. B.; Baughman, T. W.; Wagener, K. B. *J. Polym. Sci. Part A: Polym. Chem.* **2006**, *44*, 4981–4989.

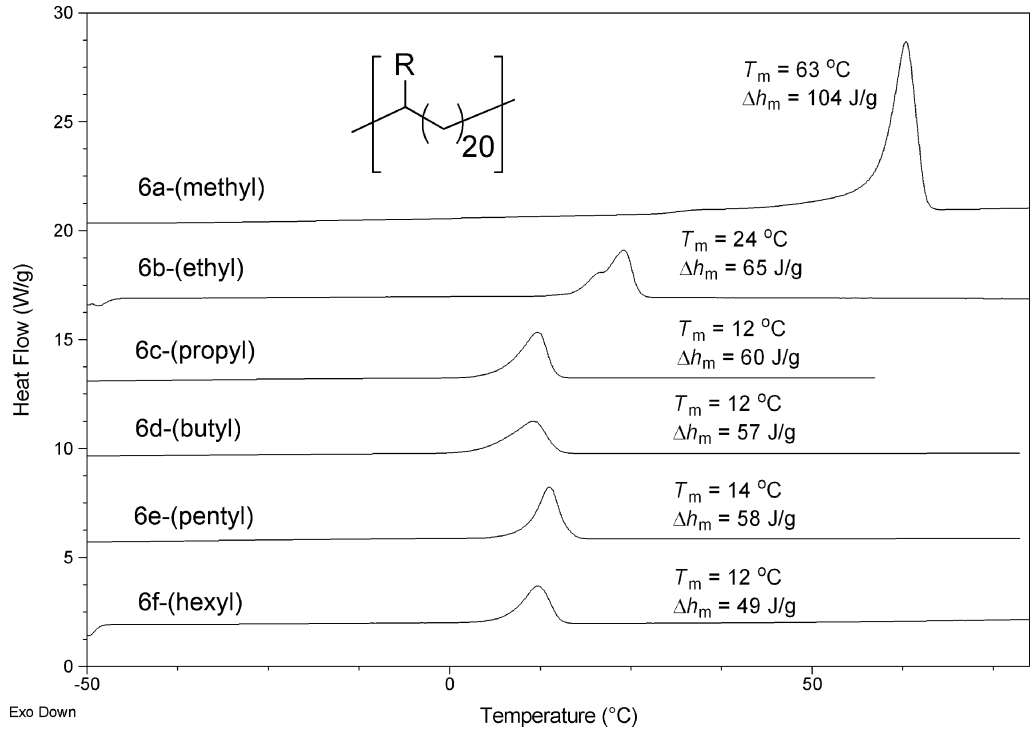

Figure 5. Differential scanning calorimetry curves for ADMET polymers possessing linear branches.

been limited, due to the heterogeneity of the material and the presence of unwanted defects.

The situation is quite different in the case of the precision branched polyolefins described here. The branch-to-branch distance is held constant, while the identity of the branch is systematically increased in size. An immediate observation becomes obvious: methyl and ethyl branching reduces the melting point of ADMET polyethylene in a progressing manner; on the other hand, all further branches, from propyl to adamantyl, produce polymers that have essentially the same melting point. There is a clear change in morphology of these polymers from a situation where the branch (methyl or ethyl) is included in the polymer's unit cell to one where branches of greater mass are excluded from the unit cell.

Figure 5 shows the DSC thermograms for the previously reported **6a-(methyl)**, **6b-(ethyl)**, **6d-(butyl)**, and **6f-(hexyl)** polymers,[43−45] along with the **6c-(propyl)** and **6e-(pentyl)** polymer models (refer to Table 1 for physical data). Similar to previous studies involving ADMET PE,[43−45] **6c-(propyl)** and **6e-(pentyl)** (i.e., polyethylene containing propyl and pentyl branches on every 21st backbone carbon) display well-defined endothermic transitions, with none of the broadening observed for analogous copolymers obtained via chain polymerization.[9,11,12,77−79]

The data in Figure 5 show that incorporation of defects precisely spaced by 20 backbone carbons causes the melting temperature of the material to decrease. While high-density polyethylene with practically no defects along the main chain shows a melting transition at $T_m = 134$ °C with a heat of fusion $\Delta h_m = 204$ J/g,[42] incorporation of methyl branches on every 21st backbone carbon, **6a-(methyl)**, decreases the melting point to 63 °C and the enthalpy of fusion to 104 J/g. This effect is explained by the disruption of the crystal structure due to the presence of the precisely placed methyl "defects". The same trend is observed when the alkyl branch is an ethyl group, **6b-(ethyl)**, as shown in Figure 5. Incorporation of an ethyl branch "defect" on every 21st backbone carbon renders a material with a melting point below that of **6a-(methyl)** ($T_m = 24$ °C with a heat of fusion $\Delta h_m = 65$ J/g). This indicates that the larger ethyl groups disrupt the crystal structure even more, resulting in depression of both the melting temperature and the heat of fusion. Even so, the branch remains in the unit cell, albeit changing its crystalline lattice. Crystal structures of both **6a-(methyl)** and **6b-(ethyl)** obtained using wide-angle X-ray diffraction (WAXD) and small-angle X-ray scattering (SAXS) reveal that the chains pack into a triclinic lattice that allows inclusion of methyl and to some extent ethyl branches as lattice defects.[44,47]

The ADMET polymers **6c-(propyl)**, **6d-(butyl)**, **6e-(pentyl)**, and **6f-(hexyl)** also give well-defined endotherms, as shown in Figure 5. Extension of the branch size from ethyl to propyl follows the same pattern of decreasing the melting temperature and heat of fusion ($T_m = 24$ °C and $\Delta h_m = 65$ J/g for **6b-(ethyl)**, $T_m = 12$ °C and $\Delta h_m = 60$ J/g for **6c-(propyl)**). However, at this point the morphology of the polymer changes significantly. Incorporation of larger branches, even adamantyl branches, leads to a series precision branched polyethylenes having very similar - in some cases identical - melting behavior, regardless of the mass of the branch. Polymers containing linear branches with three or more carbons on every 21st backbone carbon [**6c-(propyl), 6d-(butyl)**, **6e-(pentyl)**, and **6f-(hexyl)**] melt at ~13 °C with $\Delta h_m \sim 58$ J/g. Three- to six-carbon side branches are excluded from the crystal lattice, quite a different situation than for methyl and ethyl branching. It is noteworthy that the endotherm for the ethyl branched polymer, **6b-(ethyl)**, shows a shoulder on the lower melting side. This may indicate partial exclusion of ethyl branches from the unit cell such that the material may contain two types of crystalline regions.

(77) Bracco, S.; Comotti, A.; Simonutti, R.; Camurati, I.; Sozzani, P. *Macromolecules* **2002**, *35*, 1677–1684.
(78) Zhang, F. J.; Song, M.; Lu, T. J.; Liu, J. P.; He, T. B. *Polymer* **2002**, *43*, 1453–1460.
(79) Pak, J.; Wunderlich, B. *Macromolecules* **2001**, *34*, 4492–4503.

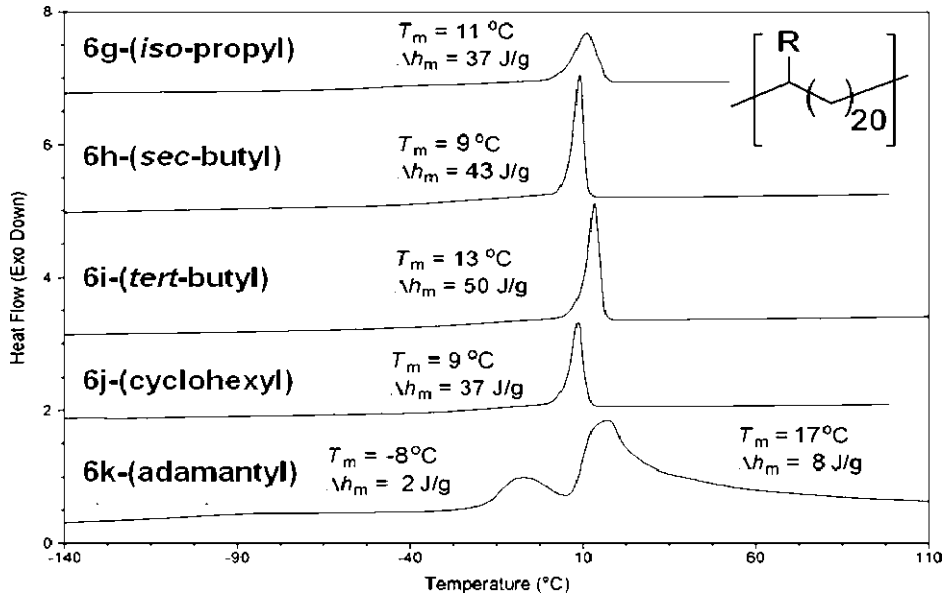

Figure 6. Differential scanning calorimetry curves for ADMET polymers possessing bulkier branches.

Similar observations are made for precision polyethylene possessing nonlinear, even bulkier branches. Data for such polymers are found in Figure 6 (also Table 1) for polymers **6g-(*iso*-propyl)**, **6h-(*sec*-butyl)**, **6i-(*tert*-butyl)**, **6j-(cyclohexyl)**, and **6k-(adamantyl)**. Melting points are similar, in the range of 9−17 °C with similar enthalpies of fusion. These homologous polymers with nonlinear bulkier branches display sharp, well-defined endothermic transitions, with none of the broadening observed for copolymers obtained via chain polymerization.[25−36]

It is interesting that polymers with bulky, nonlinear branches display much the same thermal properties as polymers with linear side chains of three or more carbons; both types of branches are excluded from the unit cell. There must be a limit in size where the side branch totally disrupts crystallization of the main PE chain. We are approaching that limit with the adamantyl branch, since the crystal lattice is quite disturbed, forcing the material to crystallize in two different domains, as evidenced by a bimodal endotherm (Figure 6). Although not shown here, annealing experiments reveal that it is possible to force the adamantyl-branched polyethylene to crystallize in one type of crystalline region by holding the sample at −20 °C for 2 h. Only one endotherm was observed at −19 °C with a Δh_m of 26 J/g.

D. X-ray Investigation for Precisely Sequenced Polymers. Wide-angle X-ray diffraction (WAXD) measurements further support the observation of a change in polymer morphology as a function of branch size. Six such WAXD diffractograms are shown in Figure 7; these patterns indicate that the introduction of branches leads to the lattice distortion and local conformational disorder, where the type of crystal structure and polymer morphology is strongly dependent on the branch identity.

For the sake of comparison, **ADMET PE** is displayed at the bottom of Figure 7 exhibiting the typical orthorhombic crystal form with two characteristic crystalline peaks superimposed with the amorphous halo, exactly the same as for high-density polyethylene made by chain propagation chemistry. The more intense peak at scattering angle 21.5° and the less intense one at 24.0° correspond to reflection planes (110) and (200), respectively. Upon introducing precisely placed branches of known identity, the crystal structure loses its symmetry with the unit cell shifting from orthorhombic to triclinic. Moreover, in contrast to linear polyethylene, scattering occurs at relatively lower scattering angles and with broader reflections being displayed, suggesting the increase of crystallite size and a decrease of crystallinity.

In the case of the methyl-branched polymers **6a-(methyl)**, two reflections representing a triclinic crystal orientation occur at scattering angle 19° with the Miller index (100) and 22° with the Miller index (010). Transmission electron microscopy (TEM) shows the lamellar thickness to be quite small, between 10 and 20 nm,[81] a thickness that can only present if the methyl side chains are incorporated in a triclinic lattice.

Similar changes in crystalline unit cell identity were observed in the ethyl branched polymer, **6b-(ethyl)**.[80] Two strong reflections shift to lower scattering angles (18° and 21°) compared to the methyl-branched polymer (19° and 22°). On the basis of Bragg's law, this observation allows us easily to draw the conclusion that the ethyl branch is incorporated in the crystal region. In contrast to the **6a-(methyl)**, the introduction of the ethyl side chain perturbs the crystal structure more and requires larger space to be incorporated. As a consequence, the reflections shift to lower scattering angles, which correspond to larger *d*-spacing.

For the polymers possessing bulkier branches (propyl or larger), the WAXD diffractograms (the top four graphs in Figure 7) show nearly identical scattering patterns, indicating that the crystal structure is independent of the branch identity. Moreover, these patterns are obviously different from those of polymers possessing smaller branches like methyl or ethyl branches, exhibiting larger scattering angles and even broader reflections.

To understand these observations, the scattering angles of two strong diffraction peaks as a function of branch identity are illustrated in Figure 8. We see two trends: the decrease of scattering angles for smaller branches, followed by leveling-

(80) Sworen, J. C. *Modeling Linear-Low Density Polyethylene: Copolymers Containing Precise Structures*. PhD Thesis, University of Florida, Gainesville, FL, 2004.

(81) Lieser, G.; Wegner, G.; Smith, J. A.; Wagener, K. B. *Colloid Polym. Sci.* **2004**, *282*, 773–781.

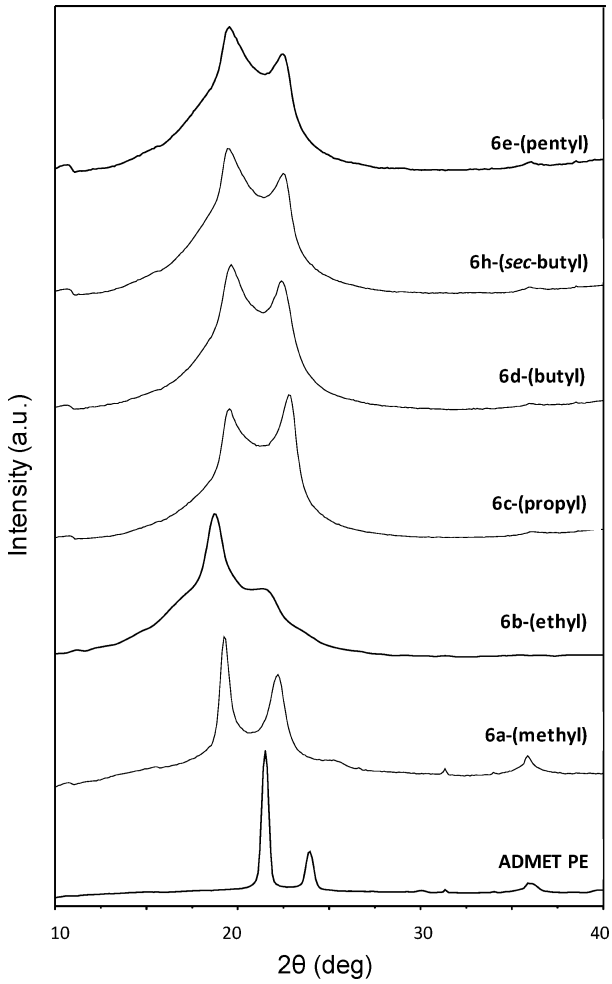

Figure 7. Wide-angle X-ray diffraction patterns for seven precision polymers: **ADMET PE** at 27 °C (no branch, T_m = 134 °C), **6a-(methyl)** at 27 °C (methyl branch, T_m = 63 °C), **6b-(ethyl)** at room temperature (ethyl branch, T_m = 24 °C),[80] **6c-(propyl)** at 0 °C (propyl branch, T_m = 12 °C), **6d-(butyl)** at 0 °C (butyl branch, T_m = 12 °C), **6h-(*sec*-butyl)** at 0 °C (*sec*-butyl branch, T_m = 9 °C), **6e-(pentyl)** at 0 °C (pentyl branch, T_m= 14 °C). Prior to measurements, all samples were heated to above melting temperature in order to remove thermal history and then cooled to specific temperature at a rate of 1 °C/min.

off of the scattering angles for bulkier branches. The former trend is easily understood. The methyl/ethyl side chains function as defects in the crystal lattice and result in the increase of *d*-spacing, thus decreasing scattering, where the ethyl results in a smaller scattering angle. Distinct difference is the case for the bulkier branches, where the angles for bulkier branched polymers, **6c-(propyl)**, **6d-(butyl)**, **6e-(pentyl)**, and **6h-(*sec*-butyl)** increase to higher degrees, 19.5° and 22.5°. Recall the X-ray scattering theory: scattering angles are determined by the type of unit cell while the peak intensities are based on the atom arrangements within the lattice. With this in mind, we conclude that the packing behaviors of precision polymers possessing sizes equal to or larger than propyl are different from those of the methyl- and ethyl-branched polymers. In all cases, the bulkier branch is excluded from the unit cell into the amorphous region. The morphology and packing behavior of these precision polymers with bulky branches are independent of the size of the branch. This assessment is in agreement with the thermal data in Table 1, where essentially identical melting temperatures are observed for all the branched polymers.

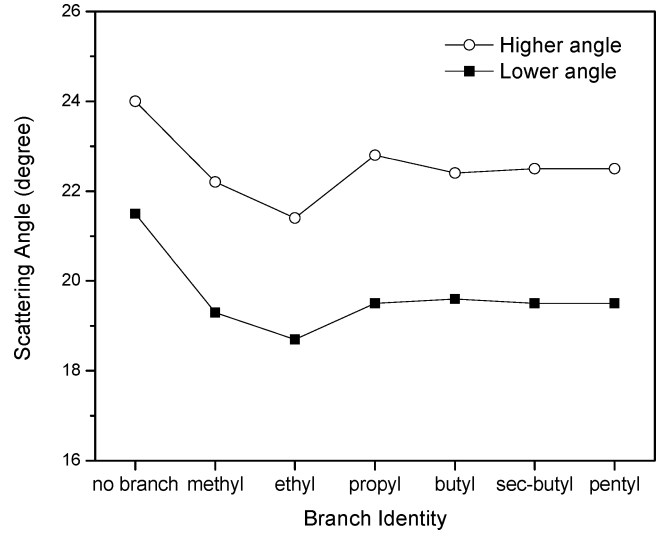

Figure 8. Scattering angles of two strong reflections for alkyl-branched precision polymers. The top graph is for the reflection at higher angle, while the bottom one is for the reflection at lower angle.

Note that the reflection occurring at ~19.5° is much broader and less symmetric than peaks for the methyl-branched polymer **6a-(methyl)** or ethyl-branched polymer **6b-(ethyl)**. The asymmetry suggests the presence of more than one crystal lattice besides triclinic; broadening is due to a decrease in the degree of crystallinity.

Of particular interest is the fact that the WAXD scattering patterns for these precision polyolefins are noticeably different from those for randomly branched polymers: the precision structures result in varying crystal lattice identity and relatively sharper scattering peaks.[47,82−85] The random ethylene−propylene (EB) copolymer with 20% comonomer content exhibits a dominant hexagonal crystal form,[83] compared to the triclinic form present in our precision **6b-(ethyl)** polymer. As for the random ethylene−butene (EB) copolymer, it shows orthorhombic crystal structure with low crystallinity.[83,84] In contrast, the precision ethylene−octene (EO) polymer (**6f-hexyl**) exhibits an additional hexagonal mesophase besides the orthorhombic crystalline phase.[85]

Conclusions

A universal two-step alkylation−decyanation synthesis procedure has been assembled to prepare a series of 11 symmetrical diene monomers where the branch is 'built-in' before the polymerization. The precise primary structures of both monomers and polymers have been confirmed via ^{1}H NMR, ^{13}C NMR, and IR spectroscopy to prove the purity of the monomers and the absence of the undesired side reactions during polycondensation and hydrogenation steps.

Thermal characterization of the polymers by DSC confirmed the precise nature of ADMET polymers by displaying sharp and well-defined endothermic transitions. Methyl and ethyl branches, being included in the unit cell, decrease the melting point of ADMET polyethylene in a progressive manner,

(82) Alamo, R. G.; Jeon, K.; Smith, R. L.; Boz, E.; Wagener, K. B.; Bockstaller, M. R. *Macromolecules* **2008**, *41*, 7141–7151.
(83) Hu, W.; Srinivas, S.; Sirota, E. B. *Macromolecules* **2002**, *35*, 5013–5024.
(84) Hu, W.; Sirota, E. B. *Macromolecules* **2003**, *36*, 5144–5149.
(85) Androsch, R.; Blackwell, J.; Chvalun, S. N.; Wunderlich, B. *Macromolecules* **1999**, *32*, 3735–3740.

lowering the melting point and degrees of crystallinity as compared with an unbranched ADMET polyethylene standard. On the other hand, increasing the size of the branch to propyl and larger yields a set of polymers with a completely different morphology; the branches are excluded from the unit cell, leaving a crystalline similar for all of them, even for the adamantyl-branched polymer. All these polymers exhibit essentially the same melting temperature and degree of crystallinity. WAXD patterns support this argument. The morphology of these precisely branched polymers changes dramatically, depending on the branch mass. Relatively smaller branches (methyl and ethyl) are included in the polymer's unit cell, whereas branches possessing greater mass and steric bulk are excluded from the unit cell.

Acknowledgment. The authors thank the National Science Foundation under grant DMR-0703261 and the International Max Planck Research School for Polymer Materials for financial support. We also thank Dr. Werner Steffen at Max Planck Institute for Polymer Research for help with the X-ray measurements.

Supporting Information Available: Experimental procedures and spectral data for all monomers and polymers. This material is available free of charge via the Internet at http://pubs.acs.org.

JA907521P